2.2   THE FALLACY OF THE ENTHALPY TRANSFER COEFFICIENT IN HIGH WINDS

Edgar L Andreas[*]
NorthWest Research Associates, Inc.
Lebanon, New Hampshire

1. INTRODUCTION

Fifteen years ago, Emanuel (1995) reported calculations of hurricane intensity based on his simple, balanced axisymmetric model of tropical cyclones. His specific objective was to build on the work by Ooyama (1969) and Rosenthal (1971) and investigate how sensitive storm intensity was to the surface exchange coefficients for enthalpy (C_K) and momentum (C_D). He summarized his findings in the following key statements:

> The direct implication of this result . . . is that the ratio C_K/C_D is most likely to lie in the range 1.2–1.5 in the high wind region of these intense storms. *In no event are the results from either model consistent with values of C_K/C_D less than about three-fourths.*

This paper was pivotal for air-sea interaction research because it focused attention on the need to better understand the physics of air-sea exchange in high winds: The data and air-sea flux parameterizations available in 1995, which treated winds up to only about 20 m s^{-1}, were not compatible with Emanuel's (1995) constraint on C_K/C_D. Theory and observations in moderate winds put C_K/C_D at values much less than 0.75 and, thus, spurred researchers to understand the discrepancy.

Emanuel's (1995) paper, however, also had some unintended adverse effects. Many inferred from it that using an enthalpy transfer coefficient is the best way to model how ocean heat influences storms and, furthermore, that the enthalpy transfer coefficient is constant—or, perhaps, a single-valued function of wind speed. These inferences have impeded progress on storm modeling because all are fallacious.

Here is a list of fallacious inferences that have been drawn from Emanuel's (1995) paper and that otherwise exist in the air-sea interaction community when the discussion involves high

---

[*]*Corresponding author address:* Dr. Edgar L Andreas, NorthWest Research Associates, Inc. (Seattle Division), 25 Eagle Ridge, Lebanon, NH 03766-1900; e-mail: eandreas@nwra.com

winds. I will address all of these here.

- C_K (and C_H, C_E) is constant (C_H and C_E are comparable transfer coefficients for sensible and latent heat).
- C_K (and C_H, C_E) is a single-valued function of wind speed.
- C_K (and C_H, C_E) should increase monotonically with wind speed when sea spray becomes a significant agent for air-sea exchange.
- C_K/C_D is constant.
- C_K/C_D is a single-valued function of wind speed.
- Observations suggest that Emanuel's (1995) guideline, $C_K/C_D \geq 0.75$, is invalid.

In high winds, when copious amounts of sea spray fill the near-surface air, two routes exist by which enthalpy crosses the air-sea interface. One is through exchange controlled by molecular processes right at the air-sea interface (the *interfacial* route); a second is through spray-mediated processes (the *spray* route). Because the two transfer processes scale differently with wind speed and other mean meteorological variables, the enthalpy transfer coefficient is not single-valued and, thus, cannot be used alone to predict the air-sea enthalpy flux in high winds.

Here, I demonstrate these ideas by using a state-of-the-art bulk flux algorithm to compute total air-sea enthalpy fluxes for a wide range of environmental conditions. That algorithm (Andreas et al. 2008; Andreas 2010) treats both interfacial and spray routes by which enthalpy crosses the air-sea interface; hence, the *total* fluxes referred to above are the sums of both contributions.

The C_K values inferred from the computed fluxes are not single-valued functions of wind speed but, rather, range over a factor of two at the lower limits of hurricane-strength winds because of a dependence on surface temperature.

The ratio C_K/C_D likewise has a spread in values for any given wind speed, and that spread increases with increasing wind speed. This C_K/C_D ratio is below Emanuel's (1995) limit of 0.75 for wind speeds between 12 and 33 m s^{-1} but rises

above 0.75 and heads toward Emanuel's preferred range of 1.2 to 1.5 for the high winds in intense storms, as he suggests.

Finally, these calculations are compatible with aircraft fluxes measured during CBLAST, the Coupled Boundary Layers and Air-Sea Transfer experiment (e.g., Black et al. 2007), and thus put in context measurements that Drennan et al. (2007) and Zhang et al. (2007) reported.

2. APPROACH

2.1 *Flux Algorithm*

For wind speeds above about 5 m s^{-1}, spray droplets are always present over the sea; and their numbers increase roughly as the third power of the wind speed (e.g., Wu 1979; Monahan and O'Muircheartaigh 1980; Monahan et al. 1986). These spray droplets provide another route by which sensible heat, water vapor, and enthalpy cross the air-sea interface.

Figure 1 shows my conceptual picture of spray-mediated transfer. Sensible and latent heat are always crossing the sea surface right at the interface. I call these the *interfacial* fluxes and denote them as H_s and H_L, respectively. In my convention, positive fluxes are upward—from sea to air.

Spray droplets provide another transfer route. The droplets originate with the same temperature as the sea surface but cool rapidly to an equilibrium temperature (T_{eq}) *below* the air temperature. In so doing, they give up sensible heat. The droplets also give up water vapor as they evaporate; but because this is a slower process, the droplets are at temperature T_{eq} for most of their evaporation. As a result, they convert sensible heat from the air to the latent heat of evaporation.

These spray processes generally take place near the sea surface in the *droplet evaporation layer* (Smith 1989; Andreas et al. 1995). A rough estimate is that this layer extends about one significant wave height above mean sea level. The total sensible and latent heat fluxes at the top of this layer, $H_{s,T}$ and $H_{L,T}$, respectively, include the contributions from both interfacial and spray transfer. The sum of these fluxes is the total enthalpy flux, $Q_{en,T}$ (e.g., Businger 1982), while the sum of H_s and H_L is the interfacial enthalpy flux, $Q_{en,int}$. The quantities $H_{s,T}$, $H_{L,T}$, and $Q_{en,T}$ can serve as the lower flux boundary conditions for atmospheric models.

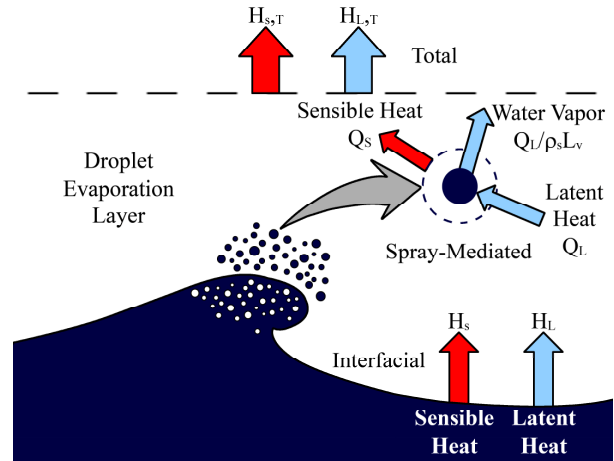Andreas et al. (2008) and Andreas (2010) developed an algorithm to estimate all of these

FIG. 1. A conceptual diagram of interfacial and spray-mediated transfer within the near-surface droplet evaporation layer. The quantities Q_S and Q_L denote radius-specific spray-mediated fluxes of sensible and latent heat, ρ_s is the density of seawater, and L_v is the latent heat of vaporization. The droplet evaporation layer is roughly one significant wave height thick. The interfacial enthalpy flux is $H_s + H_L$; the total enthalpy flux at the top of the droplet evaporation layer is $H_{s,T} + H_{L,T}$.

fluxes and tuned the algorithm with data from the experiment to study Humidity Exchange over the Sea (HEXOS) and the Fronts and Atlantic Storm-Tracks Experiment (FASTEX). In simple form, the algorithm is

$$H_{s,T} = H_s + Q_{S,sp}, \qquad (2.1a)$$
$$H_{L,T} = H_L + Q_{L,sp}, \qquad (2.1b)$$
$$Q_{en,T} = Q_{en,int} + Q_{en,sp}. \qquad (2.1c)$$

Here, $Q_{S,sp}$, $Q_{L,sp}$, and $Q_{en,sp}$ are the spray-mediated contributions to the sensible heat, latent heat, and enthalpy fluxes. Also,

$$Q_{en,int} = H_s + H_L. \qquad (2.2)$$

Because $Q_{en,sp}$ is tuned separately with the HEXOS and FASTEX data, it is close to but not always equal to $Q_{S,sp} + Q_{L,sp}$.

The flux algorithm computes the interfacial fluxes in (2.1a) and (2.1b) as (Andreas et al. 2008)

$$H_s = \rho_a c_p C_{Hr} S_r (\Theta_s - \Theta_r), \qquad (2.3a)$$
$$H_L = \rho_a L_v C_{Er} S_r (Q_s - Q_r). \qquad (2.3b)$$

Here, ρ_a is the air density; c_p, the specific heat of air at constant pressure; and L_v, the latent heat of vaporization. Also in (2.3), S_r, Θ_r, and Q_r are the effective wind speed, potential temperature, and specific humidity, respectively, at reference height r (assumed to be above the droplet evaporation layer); and Θ_s and Q_s are the sea surface values of temperature and specific humidity. The transfer coefficients for sensible and latent heat in (2.3), respectively C_{Hr} and C_{Er}, come essentially from the Coupled Ocean-Atmosphere Response Experiment (COARE) version 2.6 algorithm (Fairall et al. 1996), with a few small modifications as discussed in Andreas and Emanuel (2001), Andreas and DeCosmo (2002), Perrie et al. (2005), and Andreas et al. (2008).

Andreas et al. (2008) deduced simple parameterizations for $Q_{S,sp}$ and $Q_{L,sp}$ in (2.1a) and (2.1b):

$$Q_{S,sp} = 2.30 \times 10^{-6} \rho_s c_{ps}\left(\Theta_s - T_{eq,100}\right)u_*^3, \quad (2.4a)$$

$$Q_{L,sp} = 1.10 \times 10^{-7} \rho_s L_v \left\{1 - \left[\frac{r\left(\tau_{f,50}\right)}{50\,\mu m}\right]^3\right\}u_*^{2.22}. \quad (2.4b)$$

In these, ρ_s is the density of seawater; c_{ps}, the specific heat of seawater at constant pressure; $T_{eq,100}$, the equilibrium temperature of spray droplets that have a radius of 100 μm when they form; and $r(\tau_{f,50})$, the radius when they fall back into the sea of droplets that form with 50-μm radius. This radius comes from

$$r\left(\tau_{f,50}\right) = r_{eq,50} + \left(50\,\mu m - r_{eq,50}\right)\exp\left(-\tau_{f,50}/\tau_{r,50}\right), \quad (2.5)$$

where $r_{eq,50}$ is the equilibrium radius of droplets that form with radius 50 μm, $\tau_{r,50}$ is the e-folding time to reach that equilibrium radius through evaporation, and $\tau_{f,50}$ is the residence time in the droplet evaporation layer of droplets formed with 50-μm radius. See Andreas (2005a) for equations to calculate the quantities $T_{eq,100}$, $r_{eq,50}$, and $\tau_{r,50}$.

Lastly, in (2.4), u_* is the friction velocity, which the algorithm computes as

$$u_*^2 = C_{Dr} S_r^2. \quad (2.6)$$

Here, S_r and C_{Dr}, the drag coefficient for height r, come from the COARE version 2.6 algorithm, with the small modifications mentioned above.

In (2.3) and (2.4), the fluxes are in W m^{-2} when the other quantities have MKS units; in (2.4b) and (2.5), however, the radii are in

micrometers. In (2.6), u_* and S_r are in m s^{-1}.

From the HEXOS and FASTEX data, Andreas (2010) derived an equation similar in form to (2.4a) for the spray enthalpy flux in (2.1c):

$$Q_{en,sp} = 7.52 \times 10^{-6} \rho_s c_{ps}\left(\Theta_s - T_{eq,100}\right)u_*^{2.73}. \quad (2.7)$$

This result is consistent with Andreas and Emanuel's (2001) conclusion that, if sea spray affects the net air-sea enthalpy flux, the mechanism must be through an exchange of sensible heat.

2.2 *Implied Transfer Coefficients*

If the total enthalpy flux, (2.1c), were parameterized in terms of an enthalpy transfer coefficient C_K (i.e., under the assumption of only interfacial exchange), the expression would be (cf. Emanuel 1995)

$$Q_{en,T} = \rho_a C_{Kr} S_r \left[c_{pd}\left(\Theta_s - \Theta_r\right) + L_v\left(Q_s - Q_r\right)\right]. \quad (2.8)$$

Here, c_{pd} is the specific heat of dry air at constant pressure.

Because the Andreas (2010) algorithm computes $Q_{en,T}$ if I specify mean meteorological conditions like Θ_s, Θ_r, Q_s, Q_r, and wind speed (U_r), I can invert (2.8) to compute the implied enthalpy transfer coefficient:

$$C_{Kr} = \frac{Q_{en,T}}{\rho_a S_r \left[c_{pd}\left(\Theta_s - \Theta_r\right) + L_v\left(Q_s - Q_r\right)\right]}. \quad (2.9)$$

Ultimately, however, comparing the so-called neutral-stability transfer coefficients is more meaningful. For a standard reference height of 10 m, these values come from (e.g., Andreas and Murphy 1986)

$$C_{KN10} = \frac{k\,C_{DN10}^{1/2}}{\ln(10/r) + k\,C_{Dr}^{1/2}\,C_{Kr}^{-1} + \psi_h\left(r/L\right)}. \quad (2.10)$$

Here, k (= 0.40) is the von Kármán constant; C_{Dr} is the same value used in (2.6); C_{Kr} comes from (2.9); $\psi_h(r/L)$ is a stratification correction that appears in the near-surface temperature and humidity profiles, where L is the Obukhov length; and

$$C_{DN10}^{1/2} = \frac{k}{\ln(10/z_0)}. \quad (2.11)$$

Here, z_0 is the roughness length for wind speed from the COARE version 2.6 algorithm:

$$z_0 = 0.135\frac{\nu}{u_*} + \alpha\frac{u_*^2}{g}, \qquad (2.12)$$

where α ($= 0.0185$) is the Charnock constant, ν is the kinematic viscosity of air (in $m^2\,s^{-1}$), and g is the acceleration of gravity (in $m\,s^{-2}$). In (2.10)–(2.12), r and z_0 must be in meters.

The same set of mean meteorological variables yields $H_{s,T}$ and $H_{L,T}$ from (2.1a) and (2.1b). Hence, I can likewise obtain implied values of the neutral-stability, 10-m transfer coefficients for sensible and latent heat, C_{HN10} and C_{EN10}, under the assumption of only interfacial transfer by inverting (2.3) after first replacing H_s and H_L with $H_{s,T}$ and $H_{L,T}$, respectively. The conversions from C_{Hr} to C_{HN10} and from C_{Er} to C_{EN10} also follow (2.10).

2.3 *Parameter Space*

The final step in my approach is to generate sets of mean meteorological variables to use as input for the flux algorithm. Without losing generality and to eliminate the need to convert from height r to 10 m in (2.10), I assume that wind speed (U_{10}), air temperature (T_{10}), and relative humidity (RH) are all for a reference height of 10 m.

The Andreas et al. (2008) and Andreas (2010) algorithm is presumed reasonably accurate for U_{10} values between 5 and 40 m s^{-1}. Hence, I assign U_{10} by generating a random number between 0 and 1 and linearly mapping this to a wind speed between 5 and 40 m s^{-1}.

Likewise, I generate another random number between 0 and 1 and linearly map it to a sea surface temperature, Θ_s, between 0° and 30 °C.

I next tie the 10-m air temperature, T_{10}, to this surface temperature by assuming that $\Theta_s - T_{10}$ will always be in the interval $\Delta T_{min} = -1\,°C$ to $\Delta T_{max} = 3\,°C$. Furthermore, I assume that this interval narrows with increasing wind speed and calculate the actual sea-air temperature difference as

$$\Delta T = \left(\Delta T_{max} - \Delta T_{min}\right)\left(\frac{40-U_{10}}{40-5}\right)\gamma, \quad (2.13)$$

where γ is another random number between 0 and 1. Notice, when $U_{10} = 40$ m s^{-1}, the sea-air

temperature difference is 0 °C. I also adjust the minimum sea-air temperature difference for wind speed according to

$$\Delta T_U = \Delta T_{min}\left(\frac{40-U_{10}}{40-5}\right). \qquad (2.14)$$

This step is necessary to keep $\Theta_s - T_{10}$ referenced to 0 °C because now

$$T_{10} = \left(\Theta_s - \Delta T_U\right) - \Delta T. \qquad (2.15)$$

Lastly, I convert T_{10} to the potential temperature at 10 m, Θ_{10}.

The surface salinity of the open ocean typically is 32 to 37 psu. Again, I generate another random number between 0 and 1 and map this linearly to a salinity, S, from 32 to 37 psu. With Θ_s and S now specified, I compute Q_s as the saturation specific humidity for seawater with temperature Θ_s and salinity S.

The Andreas et al. (2008) and Andreas (2010) algorithm is formulated with relative humidity, rather than specific humidity, as the input humidity variable. Once RH is specified, however, the specific humidity at 10 m (Q_{10}) is easy to obtain.

As with air temperature, I assume that relative humidity increases with increasing wind speed. The lowest relative humidity I consider (RH_{min}) is 75%; the highest is constrained by saturation with seawater of salinity S (e.g., Roll 1965, p. 262):

$$RH_{max} = \left(1.0 - 0.000537\,S\right)\times100\%. \quad (2.16)$$

The mean relative humidity for wind speed U_{10} is thus

$$RH_{mean} = \left(RH_{max} - RH_{min}\right)\left(\frac{U_{10}-5}{40-5}\right) + RH_{min}. \quad (2.17)$$

I further assume the maximum variability about this mean humidity is ±3%. Hence, I choose the actual maximum deviation about RH_{mean} by finding another random number γ between 0 and 1 and calculating

$$\Delta RH_{max} = \left(\gamma - 0.5\right)\times6\%. \qquad (2.18)$$

Equation (2.18) centers the deviation in relative humidity around 0%. Next, I assume that this

TABLE 1. Summary of the parameter space used in calculating the neutral-stability transfer coefficients from the Andreas et al. (2008) and Andreas (2010) algorithm.

Wind Speed:	$5 \leq U_{10} \leq 40 \, \mathrm{m\,s^{-1}}$
Surface Temperature:	$0° \leq \Theta_s \leq 30°C$
Surface Salinity:	$32 \leq S \leq 37$ psu
Air Temperature:	$-1° \leq \Theta_s - T_{10} \leq 3°C$ (adjusted for wind speed)
Relative Humidity:	$75 \leq RH \leq {\sim}98\%$ (adjusted for wind speed; maximum set by S)
Barometric Pressure:	1000 mb
Water Depth:	3000 m

deviation will also decrease with increasing wind speed and calculate the relative humidity at 10 m as

$$RH = RH_{mean} + \Delta RH_{max} \left(\frac{40 - U_{10}}{40 - 5} \right). \quad (2.19)$$

Lastly, I check that RH is not less than RH_{min} and not greater than RH_{max}. If it is, I set it to the respective limit.

The Andreas et al. (2008) and Andreas (2010) algorithm also requires the barometric pressure, P, and the water depth, D. The depth occurs only in the module that computes the significant wave height, which the algorithm uses, in turn, to calculate the residence time $\tau_{f,50}$ in (2.4b) and (2.5). Because the significant wave height is not very sensitive to water depth for typical open ocean depths (Andreas and Wang 2007), I set D = 3000 m for all calculations. I likewise fix P at 1000 mb because barometric pressure only weakly influences specific humidity and air density in these calculations.

Table 1 summarizes the nominal range of all of these input variables. Andreas (2005b) gives the equations I use to evaluate the dynamic and thermodynamic quantities like ρ_a, c_p, L_v, Q_s, and Q_{10}.

The set of steps that I have just described produces one set of input variables for forcing the Andreas et al. (2008) and Andreas (2010) algorithm and, thus, yields one set of flux estimates. I repeated this sequence 2000 times to produce a reliable and representative set of fluxes and the resulting transfer coefficients.

3. RESULTS

Figure 2 shows the neutral-stability enthalpy transfer coefficient for a reference height of 10 m, C_{KN10}, that the 2000 calculations described in the last section yielded. For comparison, the figure also shows the curve that represents interfacial transfer in the Andreas et al. (2008) and Andreas (2010) algorithm. The interfacial transfer coefficient for enthalpy in neutral stability is a single-valued function of wind speed, but the implied enthalpy transfer coefficient computed from the total flux is not: C_{KN10} is a function of surface temperature and wind speed (and, less obviously, relative humidity and surface salinity).

The C_{KN10} values in Fig. 2 are approximately constant for wind speeds up to about 20 m s^{-1}. Such behavior in actual measurements of C_{KN10} (or C_{HN10} and C_{EN10}, the comparable neutral-stability transfer coefficients for sensible and latent heat) is usually interpreted to mean that sea spray has no effect on air-sea transfer (e.g., Smith 1989;
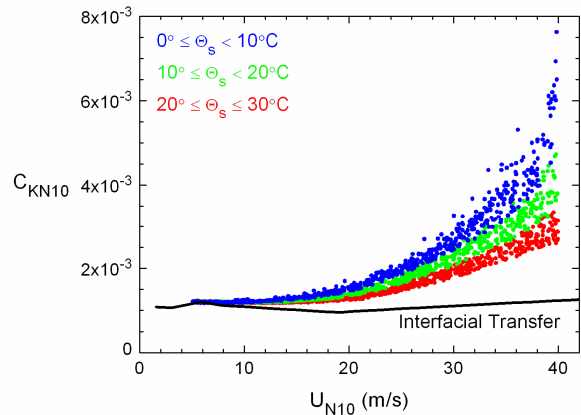

FIG. 2. Values of the neutral-stability enthalpy transfer coefficient for a reference height of 10 m, C_{KN10}, implied by the artificial data set described in Section 2 and the bulk flux algorithm (Andreas et al. 2008; Andreas 2010). The colored symbols indicate three ranges in surface temperature, Θ_s. The wind speed, U_{N10}, is the neutral-stability value at a height of 10 m. The black curve is the value that C_{KN10} would have if interfacial transfer were the only exchange mechanism.

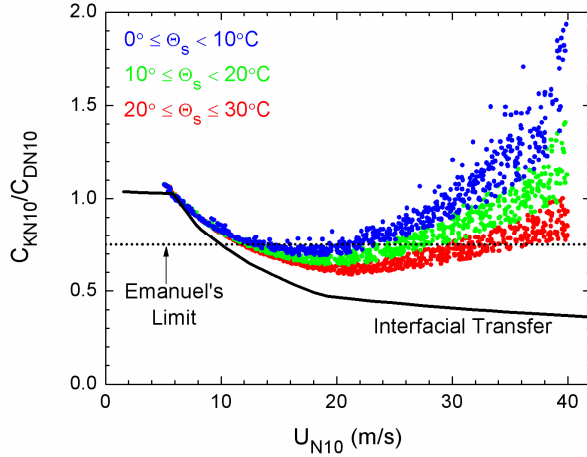FIG. 3. As in Fig. 2, except this plot shows the ratio C_{KN10}/C_{DN10}. The dashed line at 0.75 is the lowest value of C_{KN10}/C_{DN10} for which Emanuel (1995) could produce a realistic hurricane in his model.
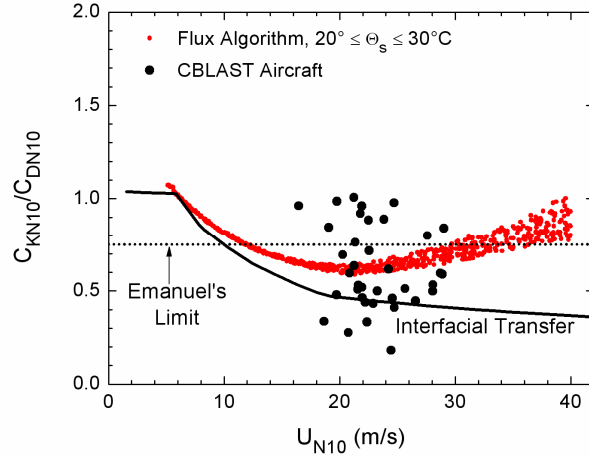

FIG. 4. As in Fig. 3, except this plot focuses on surface temperatures typical of tropical cyclones, $20° \leq \Theta_s \leq 30°C$. The black circles are from aircraft flux measurements in Hurricanes Fabian and Isabel in 2003 during CBLAST (Zhang et al. 2008).

DeCosmo et al. 1996; Smith et al. 1996). This misconception seems to go back at least to Bortkovskii (1987), who suggested in his Fig. 3.10 that the heat transfer coefficients C_{HN10} and C_{EN10} increase dramatically for winds above 15 m s^{-1} because of enhanced transfer mediated by sea spray.

Figure 2, however, suggests a different scenario. The COARE version 2.6 algorithm, which uses the surface renewal theory of Liu et al. (1979) to estimate the interfacial transfer coefficients, predicts that C_{KN10}, C_{HN10}, and C_{EN10} all decrease with increasing wind speed beyond their maxima at about 6 m s^{-1}. Thus, the transfer coefficients need not increase to reflect spray effects; the nearly constant C_{KN10} values for $5 \leq U_{N10} \leq 20 \, m \, s^{-1}$ in Fig. 2 are above the interfacial transfer limit because of spray-mediated exchange (cf. Andreas and DeCosmo 2002; Andreas et al. 2008; Andreas 2010).

Figure 3 shows what the Andreas algorithm say about the ratio C_{KN10}/C_{DN10}. Although C_{DN10} is a single-valued function of wind speed in this algorithm, C_{KN10}/C_{DN10} is not because of how spray-mediated transfer affects C_{KN10}. The figure also shows Emanuel's (1995) limit—that C_{KN10}/C_{DN10} should be larger than 0.75—and what strict interfacial transfer predicts for the value of that ratio. This interfacial curve explains why Emanuel's limit caused such concern: The C_{KN10}/C_{DN10} ratio for interfacial transfer is below

0.75 for all wind speed above about 10 m s^{-1} and is roughly half this limit for hurricane-strength winds.

Even with spray-mediated transfer, the C_{KN10}/C_{DN10} ratio in Fig. 3 is less than 0.75 for wind speeds from about 12 up to 36 m s^{-1} for some surface temperatures. Beyond this upper limit, though, C_{KN10}/C_{DN10} is greater than 0.75—a result that is entirely compatible with Emanuel's (1995) recommendation: C_{KN10}/C_{DN10} should be above 0.75 in "the high wind region" . . . of "intense storms."

Figure 4 focuses more closely on tropical cyclones. This figure repeats Fig. 3 but shows only the surface temperature range typical of tropical storms. The plot also includes aircraft measurements of C_{KN10}/C_{DN10} during the Coupled Boundary Layers and Air-Sea Transfer (CBLAST) hurricane experiment in 2003 (Zhang et al. 2008; but also French et al. 2007; Drennan et al. 2007).

Three features stand out in Fig. 4. First, most of the aircraft data are above the curve for strict interfacial transfer; thus, the CBLAST data probably document significant spray-mediated transfer. Second, predictions from Andreas's (2010) algorithm neatly cut through the CBLAST data and, thus, seem to capture the magnitude and wind speed dependencies of C_{KN10} and C_{DN10}. Third, most of the CBLAST data lie below Emanuel's (1995) limiting value of 0.75. Zhang et al. (2008) therefore concluded that Emanuel's
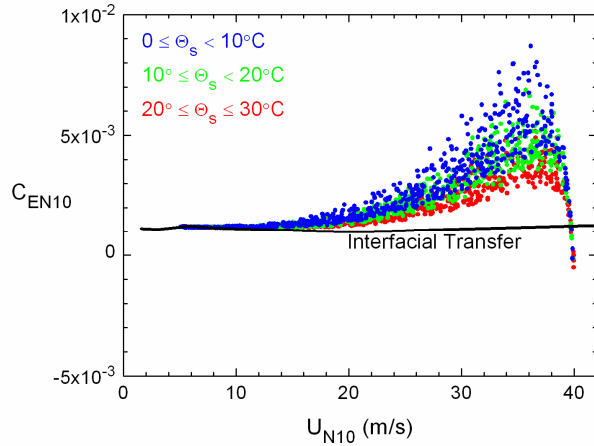
FIG. 5. As in Fig. 2, except this plot shows C_{EN10}, the neutral-stability transfer coefficient for latent heat for a reference height of 10 m.
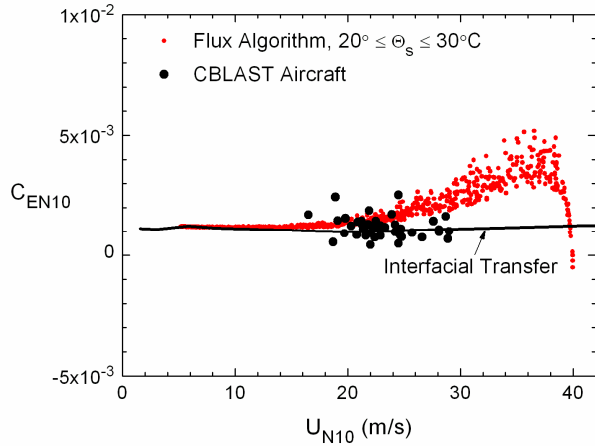

FIG. 6. As in Fig. 5, except this plot focuses on the surface temperatures typical of tropical cyclones and includes the CBLAST aircraft measurements of C_{EN10} (French et al. 2007; Drennan et al. 2007).

model needs to be "revisited." But the Andreas (2010) algorithm demonstrates that C_{KN10}/C_{DN10} values less than 0.75 are compatible with theory in the wind speed range of the CBLAST data.

Figure 5 shows algorithm predictions of the implied neutral-stability latent heat transfer coefficient for a reference height of 10 m, C_{EN10}. Again, C_{EN10} is basically constant for wind speeds up to 20 m s^{-1}, as in the HEXOS data (DeCosmo et al. 1996). Even in this range, though, C_{EN10} is not single-valued: C_{EN10} spreads out in response to the surface temperature (among other variables). And that spread increases with increasing wind speed. The curious drop in C_{EN10} for wind speeds above 38 m s^{-1} is an artifact of how I specified relative humidity as the wind approached 40 m s^{-1}.

Figure 6 reproduces from Fig. 5 just the cases for which the surface temperature is typical of tropical cyclones because the figure also shows the CBLAST C_{EN10} values measured by aircraft in Hurricanes Fabian and Isabel in 2003 (French et al. 2007; Drennan et al. 2007). These CBLAST values tend to cluster around the line representing strict interfacial transfer—a result that is a bit curious in light of Fig. 4.

The average of the CBLAST points in Fig. 6 is $C_{EN10} = 1.18 \times 10^{-3}$, and Drennan et al. (2007) ascribe an uncertainty to this average of ±25%. As a result, the data are not precise enough to rule out spray contributions.

Another reason for the different implications of Figs. 4 and 6 is that the CBLAST values of C_{DN10} used in calculating the CBLAST C_{KN10}/C_{DN10} values in Fig. 4 are generally smaller than C_{DN10} in the Andreas et al. (2008) and Andreas (2010) algorithm. This algorithm calculates C_{DN10} in (2.11) from the Charnock-like relation in the COARE version 2.6 algorithm, (2.12).

Figure 7 is the final plot in this series. It shows values of the neutral-stability, 10-m coefficient for sensible heat transfer, C_{HN10}, implied by the data set generated in Section 2. The data segregate according to the sea-air potential temperature difference, $\Delta\Theta \equiv \Theta_s - \Theta_{10}$, and their spread increases with increasing wind speed. Because of the way I selected the air temperature in Section 2—where $|\Delta\Theta|$ got smaller with increasing wind speed—the mid-range orange symbols ($1° \leq \Delta\Theta < 2°C$) in Fig. 7 extend only to about 28 m s^{-1}, and the high-range red symbols ($2° \leq \Delta\Theta \leq 3°C$) extend only up to about 15 m s^{-1}.

Because spray droplets always cool to a temperature less than the air temperature (i.e., a spray-mediated transfer of sensible heat from sea to air), the blue symbols in Fig. 7 are quite scattered. These symbols represent stable stratification ($\Delta\Theta < 0°C$), which implies a negative interfacial sensible heat flux. But the spray-mediated transfer can still be positive. Consequently, with spray-mediated transfer, the total sensible heat flux can actually be counter-gradient—a net positive heat flux despite a negative sea-air temperature difference.
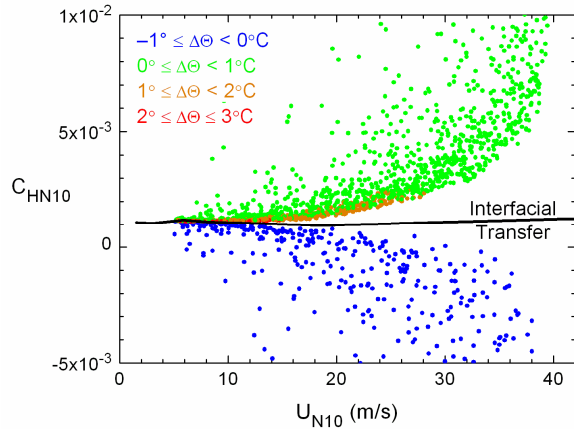
FIG. 7. Values of the neutral-stability, 10-m transfer coefficient for sensible heat, C_{HN10}, implied by the artificial data described in Section 2 and the Andreas et al. (2008) bulk flux algorithm. The colored symbols indicate four ranges in the sea-air potential temperature difference, $\Delta\Theta \equiv \Theta_s - \Theta_{10}$. The wind speed is the 10-m, neutral-stability value, U_{N10}. The black curve shows C_{HN10} for strict interfacial transfer.

The scatter in C_{HN10} in Fig. 7 caused by spray-mediated exchange may explain why measurements of C_{HN10} over the ocean are typically more scattered than measurements of C_{EN10}, especially in winds above 10 m s^{-1} (e.g., Large and Pond 1982; DeCosmo et al. 1996; Dupuis et al. 2003; Persson et al. 2005). Moreover, a main conclusion in Large and Pond (1982) is that C_{HN10} is significantly larger in unstable stratification than in stable stratification (cf. Smith 1980). Heretofore, this result has been unexplained because interfacial transfer theory predicts only minor differences between C_{HN10} and C_{EN10} and no dependence of either on atmospheric stratification. In Fig. 7, however, the average value of C_{HN10} is obviously smaller in stable stratification than it is in unstable stratification because of the spray-mediated transfer.

4. DISCUSSION AND CONCLUSIONS

Because the nature of spray-mediated air-sea transfer has only recently emerged, many earlier concepts about parameterizing air-sea heat exchange now appear fallacious. Here I have revealed several such fallacies by generating an artificial data set of mean meteorological quantities and then using a bulk flux algorithm (Andreas et al. 2008; Andreas 2010) to estimate the air-sea

fluxes of momentum, sensible heat, latent heat, and enthalpy from these data. From these input variables and the resulting fluxes, I could calculate neutral-stability, 10-m values of the drag coefficient and the transfer coefficients for sensible heat, latent heat, and enthalpy, C_{DN10}, C_{HN10}, C_{EN10}, and C_{KN10}, respectively, as if all fluxes resulted from interfacial exchange alone.

The bulk flux algorithm used to generate the fluxes parameterizes both interfacial transfer and spray-mediated transfer, however. Consequently, the resulting C_{KN10}, C_{EN10}, and C_{HN10} values do not exhibit strict interfacial scaling but, rather, are multivalued because spray-mediated heat exchange does not scale the same as interfacial exchange. To see this, compare (2.2) and (2.3) with (2.4) and (2.7). These analyses led to my conclusions that several common assumptions regarding C_{KN10}, C_{EN10}, and C_{HN10} are fallacious. I enumerate.

Although C_{KN10} and C_{EN10} may be measured as nearly constant for 10-m, neutral-stability winds (U_{N10}) less than 20 m s^{-1}, this behavior cannot be extrapolated to higher winds nor is it evidence that sea spray is playing no role in the air-sea exchanges of enthalpy and latent heat. Theory predicts that both C_{KN10} and C_{EN10} should decrease monotonically as wind speed increases from 6 to 20 m s^{-1} if interfacial transfer is the only exchange mechanism. The fact that observations of C_{KN10} and C_{EN10} do not decrease in this wind speed range is, thus, evidence of spray-mediated transfer that complements the interfacial transfer. Moreover, above $U_{N10} = 20 \text{ m s}^{-1}$, I predict that both C_{KN10} and C_{EN10} increase dramatically with wind speed because of the ever-increasing importance of spray transfer.

The behavior of the inferred C_{HN10} is more complex because spray-mediated exchange almost always leads to a sea-to-air flux of sensible heat. Interfacial sensible heat transfer, on the other hand, is always down the potential temperature gradient. Hence, sometimes the interfacial and spray fluxes are complementary, but sometimes they are in opposite directions. The two transfer routes thus lead to C_{HN10} values that are much more scattered than C_{KN10} and C_{EN10}. In fact, the opposing fluxes can lead to negative values of C_{HN10}—that is, to counter-gradient fluxes—a clear violation of strict interfacial transfer theory. As a result, I suspect that measurements of negative C_{HN10} (which are true) are often not reported because they fail to pass quality controls that require heat fluxes to be down the gradient.

Many reported measurements of C_{EN10} and

C_{HN10} over the ocean have yielded plots with some of the general features of Figs. 5 and 7. Even in modest winds (where spray is still, nevertheless, making a contribution), measured C_{HN10} values are often more scattered than measured C_{EN10} values. The explanation until now has usually been that the sensible heat flux is a weaker signal over the ocean than is the latent heat flux; the transfer coefficient for sensible heat, thus, would have a larger uncertainty and more scatter. An equally plausible explanation now is that spray-mediated transfer confounds parameterizations that presume only interfacial transfer (i.e., of C_{HN10}).

When Large and Pond (1982) segregated their C_{HN10} data into measurements in stable and unstable stratification, they found C_{HN10} to be significantly larger in unstable stratification—a result that, for them, was "neither predicted nor expected." Figure 7, however, now predicts just this result in the wind speed range up to 20 m s^{-1}, where most of Large and Pond's data fell. Meanwhile, Large and Pond and Anderson and Smith (1981) did not find a comparable dependence of C_{EN10} on stratification (cf. Fig. 5).

Many have inferred from Emanuel's (1995) modeling that C_{KN10}/C_{DN10} can be taken as a constant in hurricane models or, alternatively, that this ratio is a single-valued function of wind speed. Furthermore, many often assume that C_{KN10}/C_{DN10} must be greater than 0.75 for all wind speeds though Emanuel specifically gave this limit as a constraint only "in the high wind region" of tropical cyclones. My analyses have likewise showed these three inferences all to be fallacious.

Figure 3 shows that the theory and data tuning on which my flux algorithm (Andreas et al. 2008; Andreas 2010) is based predict C_{KN10}/C_{DN10} values that are neither constant nor single-valued functions of wind speed. This ratio spreads out with increasing wind speed because interfacial and spray-mediated enthalpy transfers scale differently with wind speed, air temperature, surface temperature, relative humidity, and surface salinity. In Fig. 3, the ratios group and spread according to surface temperature, but these other environmental conditions also contribute to the spread.

Figure 4 focuses on Emanuel's (1995) constraint of 0.75. My theory predicts that C_{KN10}/C_{DN10} is less than 0.75 in gale-force winds (U_{N10} between 12 and 30 m s^{-1}) for surface temperatures that favor tropical cyclones. But this ratio rises above 0.75 at the lower limit of hurricane-strength winds (U_{N10} of 30–36 m s^{-1}); my theory is, thus, compatible with Emanuel's guidance.

Aircraft flux measurements from CBLAST in Hurricanes Fabian and Isabel and resulting evaluations of C_{DN10}, C_{EN10}, and C_{KN10} (French et al. 2007; Drennan et al. 2007; Zhang et al. 2008) seemed incompatible with spray-mediated transfer and with Emanuel's (1995) prediction for C_{KN10}/C_{DN10} when viewed alone. But when I presented the CBLAST data in the context of my predictions for C_{KN10}/C_{DN10} and C_{EN10} in Figs. 4 and 6, those data refute neither my theory of spray-mediated transfer nor Emanuel's guidance that C_{KN10}/C_{DN10} must be larger than 0.75 in hurricane winds. In brief, the CBLAST data do not include measurements in hurricane-strength winds but fall in the wind speed range 16–30 m s^{-1}, where my theory suggests that C_{KN10}/C_{DN10} should, indeed, be below 0.75, as the CBLAST data are.

In summary, we now seem to know enough about air-sea exchange to move beyond the practice of parameterizing heat fluxes in terms of transfer coefficients that obey interfacial scaling—the gravest fallacy of all. Spray-mediated transfer is significant even in winds of only 12 m s^{-1} and does not obey interfacial scaling. Thus, no heat fluxes parameterized with C_H, C_E, and C_K can be generally accurate, especially as the wind speed increases. The interfacial and spray transfer routes must be treated separately. Free FORTRAN code, based on Andreas et al. (2008) and Andreas (2010), is available at www.nwra.comn/resumes/andreas/software.php for making these calculations.

5. ACKNOWLEDGMENTS

6. REFERENCES

Anderson, R. J., and S. D. Smith, 1981: Evaporation coefficient for the sea surface from eddy flux measurements. *J. Geophys. Res.*, **86,** 449–456.

Andreas, E. L, 2005a: Approximation formulas for the microphysical properties of saline droplets. *Atmos. Res.*, **75,** 323–345.

_____, 2005b: *Handbook of Physical Constants and Functions for Use in Atmospheric*

Boundary Layer Studies. ERDC/CRREL *Monograph* No. M-05-1, U.S. Army Cold Regions Research and Engineering Laboratory, Hanover, NH, 42 pp.

―――, 2010: Spray-mediated enthalpy flux to the atmosphere and salt flux to the ocean in high winds. *J. Phys. Oceanogr.*, **40,** 608–619.

―――, and J. DeCosmo, 2002: The signature of sea spray in the HEXOS turbulent heat flux data. *Bound.-Layer Meteor.*, **103,** 303–333.

―――, and K. A. Emanuel, 2001: Effects of sea spray on tropical cyclone intensity. *J. Atmos. Sci.*, **58,** 3741–3751.

―――, and B. Murphy, 1986: Bulk transfer coefficients for heat and momentum over leads and polynyas. *J. Phys. Oceanogr.*, **16,** 1875–1883.

―――, and S. Wang, 2007: Predicting significant wave height off the northeast coast of the United States. *Ocean Eng.*, **34,** 1328–1335.

―――, J. B. Edson, E. C. Monahan, M. P. Rouault, and S. D. Smith, 1995: The spray contribution to net evaporation from the sea: A review of recent progress. *Bound.-Layer Meteor.*, **72,** 3–52.

―――, P. O. G. Persson, and J. E. Hare, 2008: A bulk turbulent air-sea flux algorithm for high-wind, spray conditions. *J. Phys. Oceanogr.*, **38,** 1581–1596.

Black, P. G., E. A. D'Asaro, W. M. Drennan, J. R. French, P. P. Niiler, T. B. Sanford, E. J. Terrill, E. J. Walsh, and J. A. Zhang, 2007: Air-sea exchange in hurricanes: Synthesis of observations from the Coupled Boundary Layer Air-Sea Transfer Experiment. *Bull. Amer. Meteor. Soc.*, **88,** 357–374.

Bortkovskii, R. S., 1987: *Air-Sea Exchange of Heat and Moisture During Storms.* D. Reidel, 194 pp.

Businger, J. A., 1982: The fluxes of specific enthalpy, sensible heat and latent heat near the Earth's surface. *J. Atmos. Sci.*, **39,** 1889–1892.

DeCosmo, J., K. B. Katsaros, S. D. Smith, R. J. Anderson, W. A. Oost, K. Bumke, and H. Chadwick, 1996: Air-sea exchange of water vapor and sensible heat: The Humidity Exchange over the Sea (HEXOS) results. *J. Geophys. Res.*, **101,** 12,001–12,016.

Drennan, W. M., J. A. Zhang, J. R. French, C. McCormick, and P. G. Black, 2007: Turbulent fluxes in the hurricane boundary layer. Part II: Latent heat flux. *J. Atmos. Sci.*, **64,** 1103–1115.

Dupuis, H., C. Guerin, D. Hauser, A. Weill, P. Nacass, W. M. Drennan, S. Cloché, and H. C.

Graber, 2003: Impact of flow distortion corrections on turbulent fluxes estimated by the inertial dissipation method during the FETCH experiment on R/V *L'Atalante*. *J. Geophys. Res.*, **108,** C3, 8064, doi:10.1029/2001JC001075.

Emanuel, K. A., 1995: Sensitivity of tropical cyclones to surface exchange coefficients and a revised steady-state model incorporating eye dynamics. *J. Atmos. Sci.*, **52,** 3969–3976.

Fairall, C. W., E. F. Bradley, D. P. Rogers, J. B. Edson, and G. S. Young, 1996: Bulk parameterization of air-sea fluxes for Tropical Ocean-Global Atmosphere Coupled-Ocean Atmosphere Response Experiment. *J. Geophys. Res.*, **101,** 3747–3764.

French, J. R., W. M. Drennan, J. A. Zhang, and P. G. Black, 2007: Turbulent fluxes in the hurricane boundary layer. Part I: Momentum flux. *J. Atmos. Sci.*, **64,** 1089–1102.

Large, W. G., and S. Pond, 1982: Sensible and latent heat flux measurements over the ocean. *J. Phys. Oceanogr.*, **12,** 464–482.

Liu, W. T., K. B. Katsaros, and J. A. Businger, 1979: Bulk parameterization of air-sea exchanges of heat and water vapor including the molecular constraints at the interface. *J. Atmos. Sci.*, **36,** 1722–1735.

Monahan, E. C., and I. Ó Muircheartaigh, 1980: Optimal power-law description of oceanic whitecap coverage dependence on wind speed. *J. Phys. Oceanogr.*, **10,** 2094–2099.

―――, D. E. Spiel, and K. L. Davidson, 1986: A model of marine aerosol generation via whitecaps and wave disruption. *Oceanic Whitecaps and Their Role in Air-Sea Exchange Processes*, E. C. Monahan and G. Mac Niocaill, Eds., D. Reidel, 167–174.

Ooyama, K., 1969: Numerical simulation of the life cycle of tropical cyclones. *J. Atmos. Sci.*, **26,** 3–40.

Perrie, W., E. L Andreas, W. Zhang, W. Li, J. Gyakum, and R. McTaggart-Cowan, 2005: Sea spray impacts on intensifying midlatitude cyclones. *J. Atmos. Sci.*, **62,** 1867–1883.

Persson, P. O. G., J. E. Hare, C. W. Fairall, and W. D. Otto, 2005: Air-sea interaction processes in warm and cold sectors of extratropical cyclonic storms observed during FASTEX. *Quart. J. Roy. Meteor. Soc.*, **131,** 877–912.

Roll, H. U., 1965: *Physics of the Marine Atmosphere.* Academic Press, 426 pp.

Rosenthal, S. L., 1971: The response of a tropical cyclone model to variations in boundary layer

parameters, initial conditions, lateral boundary conditions, and domain size. *Mon. Wea. Rev.*, **99,** 767–777.

Smith, S. D., 1980: Wind stress and heat flux over the ocean in gale force winds. *J. Phys. Oceanogr.*, **10,** 709–726.

——, 1989: Water vapor flux at the sea surface. *Bound.-Layer Meteor.*, **47,** 277–293.

——, K. B. Katsaros, W. A. Oost, and P. G. Mestayer, 1996: The impact of the HEXOS programme. *Bound.-Layer Meteor.*, **78,** 121–141.

Wu, J., 1979: Oceanic whitecaps and sea state. *J. Phys. Oceanogr.*, **9,** 1064–1068.

Zhang, J. A., P. G. Black, J. R. French, and W. M. Drennan, 2008: First direct measurements of enthalpy flux in the hurricane boundary layer: The CBLAST results. *Geophys. Res. Lett.*, **35,** L14813, doi:10.1029/2008GL034374.